International Journal of Structural Analysis & Design– IJSAD
Volume 2: Issue 1 [ISSN : 2372-4102]
Publication Date : 30 April, 2015

External Strengthening of RC Continuous Beams Using FRP Plates: Finite Element Model

Mohammed A. Sakr, Tarek M.Khalifa, Walid N.Mansour

Abstract—Fiber reinforced polymer (FRP) installation is a very effective way to repair and strengthen structures that have become structurally weak over their life span. This paper presents a simple uniaxial nonlinear finite element model (UNFEM) able to accurately estimate the load-carrying capacity, different failure modes and the interfacial stresses of reinforced concrete (RC) continuous beams flexurally strengthened with externally bonded FRP plates on the upper and lower fibers. Results of the proposed finite element(FE) model are verified by comparing them with experimental measurements available in the literature. The agreement between numerical and experimental results is very good.This simple UNFEM is able to help design Engineers to model their strengthened structures and solve their problems.

Keywords—Continuous Beams, Debonding, Finite Element, Fibre Reinforced Polymer.

I. Introduction

Worldwide, a great deal of research is currently being conducted concerning the use of fiber reinforced plastic wraps, laminates and sheets in the repair and strengthening of reinforced concrete members. Although several research studies have been conducted on the strengthening of simply supported reinforced concrete beams using external plates, there is very less reported work on the behavior of strengthened continuous beams. Moreover, most design guidelines have been developed for simply supported beams with external FRP laminates [1]-[3]. A critical literature review revealed that a minimum amount of research work had been done for addressing the possibility of strengthening the negative moment region of continuous beam using FRP materials.

Mohamed A. Sakr
Faculty of Engineering / Tanta University
Egypt

Tarek M.Khalifa
Faculty of Engineering / Tanta University
Egypt

Walid N.Mansour
Faculty of Engineering / Kafrelsheikh University
Egypt

In the existing literature, experimental studies compare the behavior of RC continuous beams strengthened with FRP plates with the non-strengthened beam (control beam) [4]-[9]. They concluded that, the use of FRP plates/sheets to strengthen continuous beams was effective for reducingdeflections and for increasing their load carrying capacity. Aiello et al. [10] compared the behavior between continuous RC beams strengthened with carbon fibre reinforced polymers(CFRP) sheets at negative or positive moment regions and RC beams strengthened at both negative and positive moment regions. All the beams were strengthened with one CFRP sheet layer. The control beams underwent a typical flexural behavior.The failure of the strengthened beams occurred by debonding of the CFRP sheets. It was found out that when the strengthening was applied to both hogging and sagging regions, the ultimate load capacity of the beams was the highest and about 20% of moment redistribution could be achieved. Grace et al. [11] investigated the effectiveness of new tri-axially braided ductile fabric in providing ductile behaviors in RC continuous beams strengthened in flexure. They concluded that, the beams strengthened with the new fabric showed greater ductility than those strengthened with the carbon fiber sheet. Soumya Subhashree [12] tested fourteen symmetrical continuous (two-span) beams. The beams were grouped into two series. Each series have different percentage of steel reinforcement. One beam from each series was not strengthened and was considered as a control beam, whereas all other beams were strengthened in various patterns with externally bonded Glass fibre reinforced polymers (GFRP) sheets. The study concluded that, the beam was strengthened by U-wrap and was anchored by using steel plate and bolt system, showed the highest ultimate load. The percentage increase of the load capacity of that beam was 61.92 %. The load carrying capacity of beam which was strengthened by four layers of U-wrap in positive moment zone was near to the load capacity of beam strengthened by two layers U-wrap and anchored by using steel plate and bolt system. The percentage increase of load carrying capacity of that beam was 59.61 %. Using of steel bolt and plate system is an effective method of anchoring the FRP sheet to prevent the debonding failure. Strengthening of continuous beam by providing U-wrap of FRP sheet isalso an effective way of enhancing the capacity of load carrying.

Previous FE studies of FRP-strengthened beams involve the use of refined FE meshes of two-dimensional plate/shell elements [13]-[16] or three-dimensional solid elements [17] using many commercial finite element packages. Using commercial numerical finite element package Abaqus, Obaidat

et al. [18], suggested a 3D finite element model to analysis plate end interfacial debonding in retrofitted RC simple beams. Nonlinear cohesive bond model under mode-II conditions was used for the concrete–FRP interface. The high computational cost of structural response analyses based on FE models such as the ones referred above has prompted the development of purely numerical methods (not based on mechanics) for the analysis and design of FRP-strengthened RC structures [19]. Kadhim [20] focused on the behavior of the high strength concrete continuous beam strengthened with different CFRP sheet lengths, ANSYS program was used.The agreement between the results obtained from analysis and experimental date is good respect to load–deflection curve, ultimate strength, and the crack patterns. Full bond between RC beam and CFRP laminates was assumed besides neglecting the softening behavior of concrete either in compression or in tension. The length of CFRP sheet was changed in the negative and positive regions and the results showed that the ultimate strength of the beam was reached when the value of Lsheet/Lspan reaches 1.0.

Using Near Surface Mounted (NSM) strengthening technique to strengthen reinforced concrete (RC) members using FRP composites is commonly spread in recent years. Hawileh [21] presented 3D nonlinear FE numerical model that can accurately predict the load-carrying capacity and response of RC beams strengthened with NSM FRP rods subjected to four-point bending loading. The developed FE model is created using the FE code ANSYS. The developed FE model considers the nonlinear constitutive material properties of concrete, yielding of steel reinforcement, cracking of the filler bonding materials, bond slip of the steel and NSM reinforcements with the adjacent concrete surfaces, and bond at the interface between the filling materials and concrete. The numerical FE simulations were compared with experimental measurement tested by other researchers. Overall, the predicted FE mid-span deflection responses agreed very well with the corresponding measured experimental tested data at all stages of flexural loading. Furthermore, the developed models were also capable of predicting the failure mode of the strengthened tested specimen such as NSM rod debonding (peeling off) and concrete cover separation.

Although many researches carried out to understand and model debonding failure modes, it is still a very active field of research, mainly due to the complexity of the problem at hand. After hard searching in literature, the authors found that there is no analytical solution models the non-linear mode-I and mode-II fracture responses of the cohesive interface of strengthened RC continuous beams with FRP plate or strips. Here is the importance of current work appear.

The research work presented in this paper develops a new UNFEM able to simulate the mechanical behavior of FRP-strengthened RC continuous beams utilizing realistic nonlinear constitutive relations for each strengthened beam components. The interfacial shear and normal stresses in the adhesive layer are presented using analytical uncoupled cohesive zone model based on nonlinear fracture mechanics.

II. Finite Element Modeling

As shown in Fig. 1, there are three components in a strengthened beam for the present analysis model, i.e. reinforced concrete, FRP, and adhesive. The adhesive layer is modeled as contact layer generalized to handle cohesive forces in both the normal and tangential directions. Fig. 2 shows interfacial shear and normal stress distribution in the adhesive layers or in the cohesive zone. In the current study, a 21-node element is developed to represents the strengthened reinforced concrete beam as shown in Fig. 3. The reinforced concrete beam and FRP layer are modeled as beams with Euler-Bernoulli kinematics assumptions. Linear geometry due to small deformations and displacements is assumed. The cohesive zone model is utilized for determining the normal and tangential stiffness of the adhesive layer. Realistic nonlinear constitutive models are employed to represent the stress-strain behavior of concrete, reinforcing steel and bonded FRP. Perfect bond is assumed between the concrete and reinforcing steel. The model proposed in this study uses the constitutive laws of materials in the total form and not in the incremental form usually adopted in problems involving nonlinear analysis.

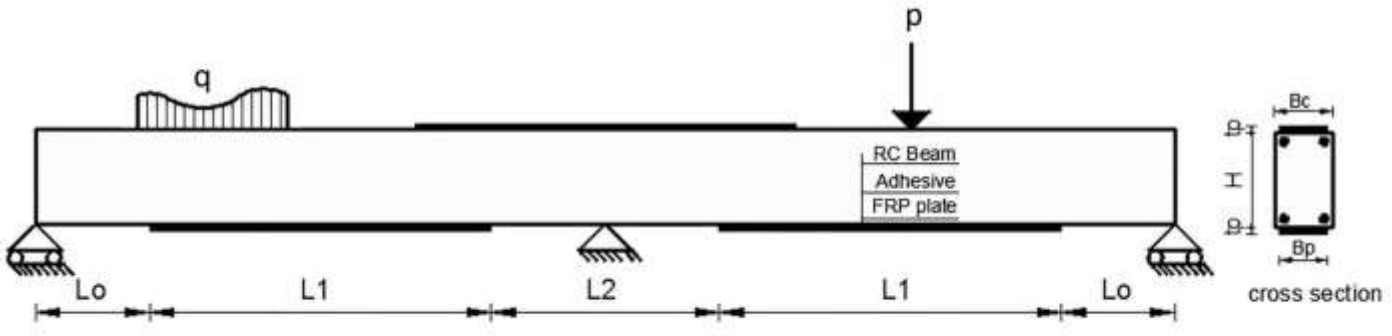

Figure 1.RC beam bonded with FRP plate

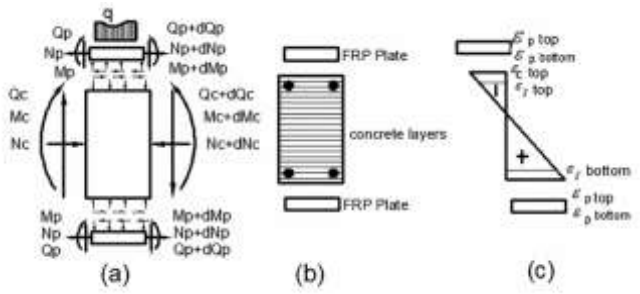

Figure 2. (a) Differential element along span; (b) general cross section geometry and layer discretization; and (c) strain distribution

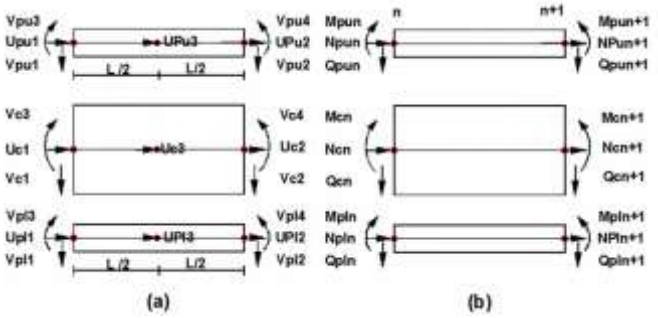

Figure 3. The developed finite element: (a) nodal degrees of freedom; (b) nodal forces

III. Constitutive Equations of Materials

A layered model approach was followed during the development of the proposed finite element for the concrete beam cross section. The cross section was divided into a finite number of layers. The layered model approach is relevant for the formulation of this type of complex elements due to (i) the difference between the properties of beam reinforcement and concrete; and (ii) the dissimilarity between the behavior of concrete in tension and compression. For concrete in compression, the stress- strain relationship suggested by [22] is adopted. This relationship is characterized by linear-elastic behavior up to 40% of the maximum strength. Beyond the elastic limit, an elastic- plastic with final softening branch is assumed. For concrete in tension, linear-elastic behavior is considered up to the cracking phenomenon, which occurs when the tensilestrength is reached. The tension stiffness of concrete between cracks due the presence of reinforcement is taken into account by the nonlinear softening law proposed by [23]. Compared to the case of concrete without reinforcement, the tensile stress does not vanish for large strain, but it tends to a positive value that depends on the percentage of reinforcement in the concrete beam. For reinforcement steel, an elastic-plastic with small hardening law typically used for structural steel has been assumed.The FRP is modeled with linear elastic-brittle behavior in tension and zero-strength and stiffness in compression.Due to its simplicity, cohesive zone modeling is largely used for behavior of adhesive layers. The energy release rates in mode-I (G_I) and mode-II (G_{II}) are identified as the areas under the respective cohesive laws integrated up to the current values of stresses. The total energy release rate is the sum of G_I and G_{II}. Different approaches have been used in the literature for cohesive zone modeling of interfaces under mixed-mode conditions:

In uncoupled cohesive zone approach, cohesive laws in the normal and tangential directions are independent from each other.

In coupled cohesive zone approach, cohesive laws in the normal and tangential directions are linked to each other, typically by means of a coupling parameter.

In the current study, uncoupled cohesive laws are considered both in the normal and tangential directions.This choice is made to enable the use of different values for the mode-I and mode-II interfacial fracture energies, in agreement with the experimental evidence. The cohesive laws implemented herein are bilinear. This simple shape is able to capture the three characteristic parameters of the interface, i.e., the fracture energies (areas underneath the curves), the cohesive strengths, and the linear-elastic properties (slopes of the curves in the ascending branch).

Following the approach given by [24], the energy release rates in mode-Iand mode-IIare identified as the areas under the respective cohesive laws integrated up to the current values of normal and tangential displacements and the simplest possible mixed-mode failure criterion . The mode-mixities can be estimated directly from the numerical predictions by examining the value of G_{II}/G_I for a crack-tip cohesive zone element just before it fails. The above cohesive models have been implemented into a 21-node composite element proposed by the current study, and generalized to handle cohesive forces in both the normal and tangential directions. Also, all the above constitutive equations of materials for concrete in tension or compression, reinforcement, and FRP have been implemented in that element.

IV. Element Formulation

With reference to the parameters of the nodal displacements of the element shown in Fig. 3, the following relationships could be written:

$$u_{pl}(x) = \mathbf{N}_p \,.\, \mathbf{U}_{\mathrm{pl}} \;; \qquad u_{pu}(x) = \mathbf{N}_p \,.\, \mathbf{U}_{\mathrm{pu}}$$

$$u_c(x) = \mathbf{N}_c \,.\, \mathbf{U}_{\mathrm{c}} \;; \qquad v_{pl}(x) = \mathbf{N}_{vp} \,.\, \mathbf{V}_{\mathrm{pl}} \;;$$

$$v_{pu}(x) = \mathbf{N}_{vp} \,.\, \mathbf{V}_{\mathrm{pu}} \;; \quad v_c(x) = \mathbf{N}_{vc} \,.\, \mathbf{V}_{\mathrm{c}} \quad (1)$$

where c, pl, and pu are subscripts relating the symbol to the centroid of reinforced concrete beam and the centroid of lower and upper FRP plates, respectively; $\mathbf{U}^T = [u_1,\ u_2,\ u_3]$ is the vector of the nodal horizontal displacements; and $\mathbf{N} = [N_1(x),\ N_2(x),\ N_3(x)]$ is the vector of the corresponding shape functions. Analogously $\mathbf{V}$ is the vector of vertical nodal displacement and $\mathbf{N}_V$ is the vector of corresponding shape functions. The tangent displacement (horizontal slip) $g^T(x)$ and normal displacement (vertical

separation) $g^N(x)$ could be written as:

A. Lower Part

$$g^T{}_l(x) = -\mathbf{N}_c\ \mathbf{U}_c + \mathbf{N}_p\ \mathbf{U}_{pl} + (H/2)\mathbf{N}'_{vc}\ \mathbf{V}_c + (t_{pl}/2)\mathbf{N}'_{vp}\ \mathbf{V}_{pl} \quad (2)$$

$$g^N{}_l(x) = -\mathbf{N}_{vc}\ \mathbf{V}_c + \mathbf{N}_{vp}\ \mathbf{V}_{pl} \quad (3)$$

B. Upper Part

$$g^T{}_u(x) = \mathbf{N}_c\ \mathbf{U}_c - \mathbf{N}_p\ \mathbf{U}_{pu} + (H/2)\mathbf{N}'_{vc}\ \mathbf{V}_c + (t_{pu}/2)\mathbf{N}'_{vp}\ \mathbf{V}_{pu} \quad (4)$$

$$g^N{}_u(x) = \mathbf{N}_{vc}\ \mathbf{V}_c - \mathbf{N}_{vp}\ \mathbf{V}_{pu} \quad (5)$$

where $\mathbf{N}'_{vc}$ and $\mathbf{N}'_{vp}$ are the first derivative of the matrix $\mathbf{N}_{vc}$ and $\mathbf{N}_{vp}$, respectively.

The studied problem is nonlinear and could be solved through iterations. Applying the principle of virtual work to a certain element for a specific iteration j yields:

$$\begin{aligned}&\int_{v_c} \delta\varepsilon_c \sigma_c^j\, dV_c + \int_{v_{pl}} \delta\varepsilon_{pl}\, \sigma_{pl}^j\, dV_{pl} + \int_{v_{pu}} \delta\varepsilon_{pu}\sigma_{pu}^j\, dV_{pu} \\ &+ B_{pl}\int_L \delta g_l^T\, p_l^T dx + B_{pl}\int_L \delta g_l^N\, p_l^N dx + B_{pu}\int_L \delta g_u^T\ p_u^T\, dx \\ &+ B_{pu}\int_L \delta g_u^N\, p_u^N dx = \int_L \delta\mathbf{V}_c\, q\, dx + \sum_i \delta\mathbf{V}_{ci}\, P_i\end{aligned} \quad (6)$$

where q and P are the distributed and concentrated load applied to the element; and v_c represents the volume of concrete and reinforcement; and v_{pl}, v_{pu} represents the volume of lower and upper FRP plates respectively. Incorporating the constitutive relations given in the previous section, as in (6), the element response is obtained by integrating the virtual work expression using three Gaussian integration points. Gauss points are normally sufficient over the element length, with several layers over the element thickness, chosen according to the required accuracy. For a generic beam made up of multiple elements, the following system of linear algebraic equations is obtained after assembling the global stiffness matrix and applying the boundary conditions:

$$\underline{\mathbf{K}}^j \cdot \underline{\mathbf{U}}^j = \underline{\mathbf{F}}^j \quad (7)$$

where $\underline{\mathbf{K}}^j$, $\underline{\mathbf{U}}^j$, $\underline{\mathbf{F}}^j$ are the stiffness matrix, the vector of unknown nodal displacements, and the load vector including all nodal forces, respectively for iteration J.

For the solution algorithm and convergence, the secant method is adopted to determine the unknown deformations considering the origin point as a base point for all secant models. The solution technique is implemented in a computer program using C++ language.

V. Experimental Validation

A. Prediction of Ultimate Load-Carrying Capacity

The proposed FE model is evaluated through a comparison between the experimentally measured and the numerically predicted load-carrying capacity of the two spansymmetrical continuousbeams included in the experimental database. The geometric properties of the specimens and the most important mechanical properties of the used materials, including both reference (i.e., non-strengthened) and FRP-strengthened beams as in [6], [7], and [12]and mostly obtained through steel coupon and FRP tensile tests or concrete compression tests.

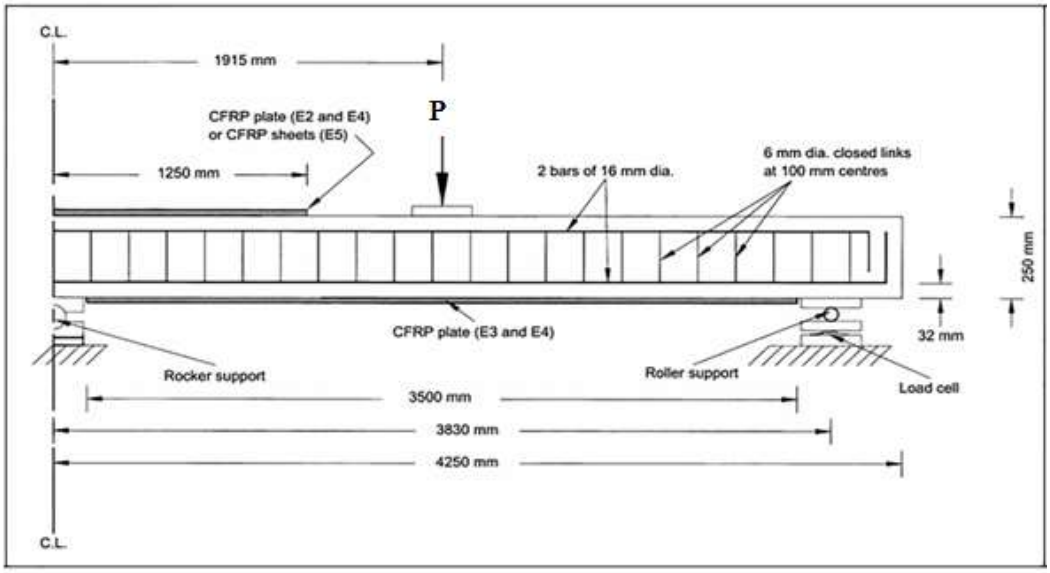

Figure 4. Geometric properties of the specimens tested in [6]

Table I and Table IIshow a comparison between the experimental ultimate load capacity, P_{exp},ultimate negative bending moment, M^{-}_{exp} ,and ultimate positive bending momentM^{+}_{exp} at failure of test specimens and the predicted FE ultimate load capacity P_{FE}, ultimate negative bending moment, M^{-}_{FE} ,and ultimate positive bending moment M^{+}_{FE} obtained by UNFEM at failure of test specimens. The ratio between the predicted and the experimental ultimate load capacity ranges from 0.93 to 1.17. The ratio between the predicted and the experimental ultimate negative bending moment ranges from 0.84 to 1.18. The ratio between the predicted and the experimental ultimate positive bending moment ranges from 0.83 to 1.16. The agreement between the experimental results and the predicted results is very good for the reference beams and the strengthened beams.

TABLE I
COMPARISON BETWEEN EXPERIMENTAL RESULTS AND NUMERICAL RESULTS OF LOAD-CARRYING CAPACITY OF REFERENCE RC BEAMS (WITHOUT FRP REINFORCEMENT)

Authors	ID	P_{exp} (kN)	P_{FE} (kN)	P_{FE}/P_{exp}	M^{-}_{exp} (kN.m)	M^{-}_{FE} (kN.m)	M^{-}_{FE}/M^{-}_{exp}	M^{+}_{exp} (kN.m)	M^{+}_{FE} (kN.m)	M^{+}_{FE}/M^{+}_{exp}	Failure mode
Ashour et al. [7]	H_1	138	137.2	0.99	21.21	23.89	1.12	56.78	53.73	0.95	Flexure
	S_1	83.6	86.20	1.03	57.77	55.00	0.95	11.13	13.77	1.23	Flexure
	E_1	149.7	148.2	0.99	54.49	48.95	0.90	44.41	46.47	1.04	Flexure
Soumya. [12]	CB_1	260	256.2	0.99	-	29.24	-	-	17.41	-	Flexure
	CB_2	200	194.2	0.97	-	13.39	-	-	17.58	-	Flexure

TABLE II
COMPARISON BETWEEN EXPERIMENTAL RESULTS AND NUMERICAL RESULTS OF -CARRYING CAPACITY OF FRP-STRENGTHENED RC BEAMS

Authors	ID	P_{exp} (kN)	P_{FE} (kN)	P_{FE}/P_{exp}	M^{-}_{exp} (kN.m)	M^{-}_{FE} (kN.m)	M^{-}_{FE}/M^{-}_{exp}	M^{+}_{exp} (kN.m)	M^{+}_{FE} (kN.m)	M^{+}_{FE}/M^{+}_{exp}	Failure mode
Ashour et al. [7]	H_2	152.3	165.2	1.08	31.60	34.81	1.10	61.00	61.68	1.01	TR
	H_3	172.9	180.2	1.04	46.48	51.20	1.10	59.56	60.66	1.01	PF
	H_4	162.6	191.2	1.17	53.07	63.11	1.18	51.32	59.97	1.16	PF
	H_5	162.6	153.2	0.94	35.00	40.48	1.15	64.27	53.1	0.83	PF
	H_6	172.9	161.2	0.93	28.26	35.58	1.17	70.24	60.57	0.86	PF
	S_2	121.8	119.2	0.98	71.28	61.24	0.86	22.67	26.45	1.16	SS
	S_3	121.8	121.2	0.99	66.90	61.24	0.92	24.72	27.4	1.10	PF*
	S_4	170.5	166.2	0.97	88.97	65.3	0.84	37.15	42.17	1.15	PF*
	S_5	111.7	115.2	1.03	50.18	45.19	0.90	28.36	32.55	1.14	SS
	E_2	178.6	175.2	0.98	79.78	75.83	0.95	45.64	45.96	1.00	PF
	E_3	207.0	223.2	1.07	53.56	48.10	0.90	72.35	82.8	1.14	PF*
	E_4	231.4	222.2	0.96	77.00	77.78	1.01	72.29	67.48	0.93	PF
	E_5	174.6	175.2	1.0	77.42	75.75	0.98	44.87	45.99	1.02	PF
Soumya. [12]	SB1	320	295.2	0.93	-	35.74	-	-	19.03	-	PF
	TB1	224	223.2	0.99	-	18.34	-	-	18.73	-	PF

TR= Tensile rupture of the CFRP sheets over the central support followed by flexural failure, PF= Peeling failure (Debonding over the central support), SS=Sheet separation (under concentrated load), PF*= Peeling failure (under concentrated load).

B. Comparison of Load-Deflection Response

This study carried out also a comparison between experimentally recorded and numerically simulated applied load-midspan deflection response of reference and FRP-strengthened beams. Only few of database studies contain also the applied load-midspan deflection responses of the tested specimens. Here, the results corresponding to the study presented in [6] are shown and described in detail. The geometric properties of the test specimens are shown in Fig. 4. Fig. 5 plots the applied load - midspan deflection responses for the reference beam specimen and FRP-strengthened beam specimens. The agreement between numerical simulations and experimental records is excellent for the reference beam and very good for the FRP-strengthened beams.

C. Comparison of Hogging and Sagging Bending Moments

Fig. 6 plots the applied load – hogging and sagging bending moment's results for the reference beam specimen and FRP-strengthened beam specimens. The agreement between

numerical simulations and experimental records is excellent for the tested beams.

D. Comparison of Failure Modes

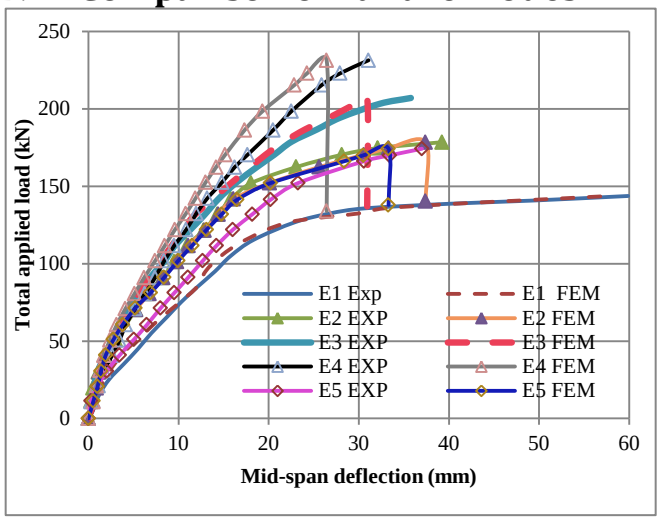

Figure 5. Comparison between experimental measurement and FE simulation of the applied force-midspan deflection response for the tests presented in [6]

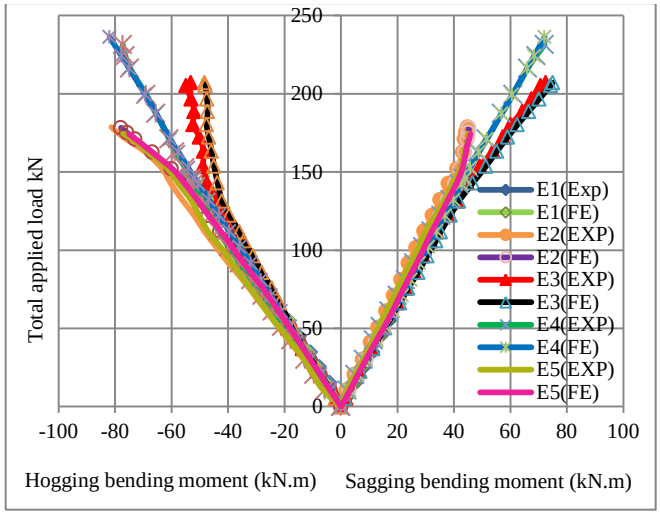

Figure6. Comparison between experimental measurement and FE results of the hogging and sagging bending moments for the tests presented in [6]

Numerical and experimental records showed that the reference beam failed in a ductile manner because of concrete crushing after large deformations while the other four strengthened beams failed as a result of a peeling failure of the concrete cover adjacent to the external CFRP reinforcement.Fig.7 shows the interfacial shear stress along beam E2 top surface FRP at different loads till failure. At total load 130.20 kN (before cracking) there is no peeling failureoccurred and the shear stress in FRP is lower than its maximum strength $p^{T}max$ (3.0 MPa). After cracking load (155.20 kN) the shear stress in FRP increased significantly till failure (178.20 kN). Fig.7 shows that peeling started at centralsupport where maximum stresses are concentrated then propagated to the beam end.Fig.8 shows the interfacial shear stress along beam E3 bottom surface FRP at different loads till failure. At total load 100.20 kN (before cracking) there is no peeling failure occurred and the shear stress in FRP is lower than its maximum strength (3.0 MPa). After cracking load (185.20 kN)the shear stress in FRP increased significantly till failure (208.20 kN). Fig.8 shows that peeling started at mid-span where maximum stresses are concentrated then propagated to the beam end.

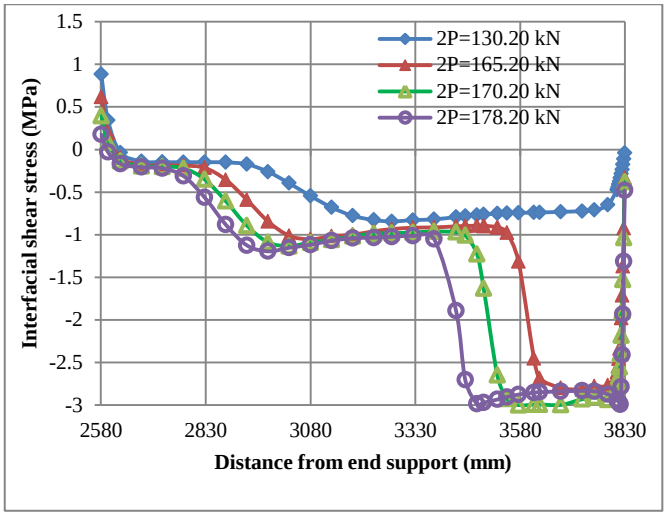

Figure7. Interfacial shear stress of the adhesive layer of upper FRP plate of beam E2 at different loads till failure

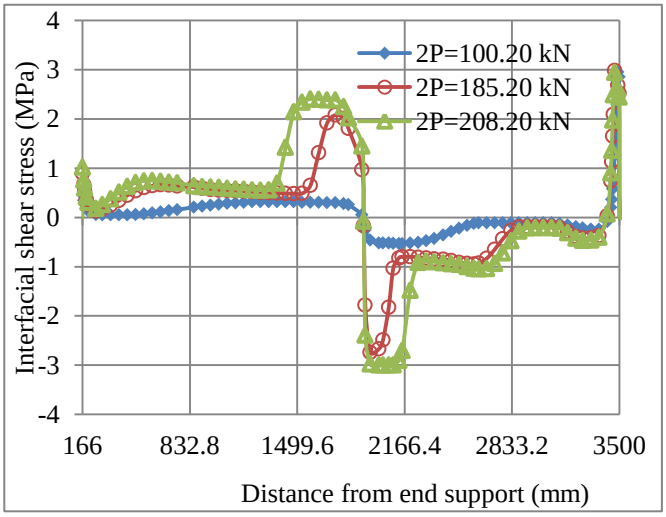

Figure8. Interfacial shear stress of the adhesive layer of lower FRP plate of beam E3 at different loads till failure

VI. Conclusion

The research work presented in this paper develops a new uniaxial nonlinear finite element model (UNFEM) able to simulate the mechanical behavior of FRP-strengthened RC continuous beams utilizing realistic nonlinear constitutive relations for each strengthened beam components. The interfacial shear and normal stresses in the adhesive layer are presented using analytical uncoupled cohesive zone model based on nonlinear fracture mechanics. The following are advantages of using the proposed UNFEM: (i) accurately

predict the ultimate load of FRP-strengthened RC beams, (ii) provides a sound mechanical description and interpretation for failure modes of FRP-strengthened RC beams, (iii) allows reducing the complexity and computational cost of FE analyses based on existing FE models, and (iv) simulates the structural response of the considered structural systems with accuracy satisfactory for practical applications.

References

[1] ACI 440, Guide for the design and construction of externally bonded FRP systems for strengthening concrete structures. Technical Report, American Concrete Institute. 2002.
[2] CEB-FIB Model Code 90, Thomas Telford Eds., London, 1993.
[3] JSCE , Recommendations for upgrading of concrete structures with use of continuous fiber sheets. Technical Report, Research Committee on Upgrading of Concrete Structures with Use of Continuous Fiber Sheets, Japanese Society of Civil Engineers.,2000.
[4] N. F. Grace, G. A. Sayed, A. K. Soliman and K. R. Saleh "Strengthening Reinforced Concrete Beams Using Fiber Reinforced Polymer (FRP) Laminates" ACI Structural Journal. pp. 865-875., September-October 1999.
[5] Grace NF . "Strengthening of negative moment region of RC beams using CFRP strips." ACI Structural Journal. vol. 3. No. 98. pp.347-358., 2001.
[6] El-Refaie, S.A., Ashour, A.F and Garrity, S.W. ,"CFRP strengthened continuous concrete beams," in Proceedings of the Institution of Civil Engineers. Structures and buildings, Vol. 156, No. 4, pp. 395–404., 2003.
[7] Ashour, A.F., El-Refaie, S.A and Garrity, S.W., "Flexural strengthening of RC continuous beams using CFRP laminates," in Cement and Concrete Composite, vol. 26, No. 7, pp. 765–775., 2004.
[8] Maghsoudi AA, and Bengar H, "Moment redistribution and ductility of RHSC continuous beams strengthened with CFRP", Turkish Journal of Engineering and Environmental Sciences, vol. 33, pp. 45-59, 2009.
[9] M. Rahman and M.Jumaat., , "The Effect of CFRP laminate length for strengthening the tension zone of the reinforced concrete T-beam", Journal of scientific research & reports ,vol. 2, No. 2,pp. 626-640, 2013.
[10] M. A. Aiello, L. Valente, and A. Rizzo, "Moment redistribution in continuous reinforced concrete beams strengthened with carbon-fiber-reinforced polymer laminates," Mechanics of composite materials, Vol. 43, No. 5, pp.453-466., 2007.
[11] Grace , NF., Wael, R., and Sayed, AA, "Innovative triaxially braided ductile FRP fabric for strengthening structures", 7th International Symposium on Fiber Reinforce Polymer for Reinforced Concrete Structures, ACI, Kansas City, MO, 2005.
[12] Soumya ,S. "Strengthening of RC continuous beam using FRP sheet," Department of Civil Engineering, National Institute of Technology Rourkela, Odisha, India., 2012.
[13] Jerome, D.M. and Ross, C.A. , "Simulation of the dynamic response of concrete beams externally reinforced with carbon-fiber reinforced plastic," Computers and Structures, Vol. 64, No. 5-6, pp.1129–1153.,1997
[14] Moller, B., Graf, W., Hoffmann, A. and Steinigen, F., "Numerical simulation of RC structures with textile reinforcement," Computers and Structures, Vol. 83, pp. 1659–1688., 2005.
[15] Camata, G., Spacone, E. and Zarnic, R. ,"Experimental and nonlinear finite element studies of RC beams strengthened with FRP plates," Composites, Part B Vol. 38, pp. 277–288., 2007.
[16] Zhang L. and Teng, J.G., "Finite element prediction of interfacial stresses in structural members bonded with a thin plate," Engineering Structures, Vol. 32, pp.459-471., 2010.
[17] Kotynia, R., Baky, H.A., Neale, K.W. and Ebead, U.A., "Flexural strengthening of RC beams with externally bonded CFRP systems: test results and 3D nonlinear FE analysis, " Journal of Composite Construction ASCE, Vol. 12, No. 2, pp.190–201., 2008.
[18] Obaidat, Y. T., Heyden, S. and Dahlblom, O., "The effect of CFRP and CFRP/concrete interface model when modeling retrofitted RC beams with FEM," Computers and Structures, Vol. 92, pp.1391–1398., 2010.
[19] Flood, I., Muszynski, L. and Nandy, S. ,"Rapid analysis of externally reinforced concrete beams using neural networks," Computers and Structures, Vol. 79,pp. 1553–1559., 2001.
[20] Kadhim, "Effect of CFRP Sheet Length on the Behavior of HSC Continuous Beam", Journal of Thermoplastic composite materials, Vol. 00, 2011.
[21] Rami A. Hawileh, ''Nonlinear finite element modeling of RC beams strengthened with NSM FRP rods,'' Journal of Construction and Building Materials, Vol.27, No. 1, pp.461-471, 2012.
[22] Mander, J. B., Priestley, M. J. N. and Park, R., "Theoretical stress-strain model for confind concrete," Journal of Structural Engineering (ASCE), Vol. 114, No. 8, pp.1804–1826., 1998.
[23] Stevens, N. J., Uzumeri, S. M., Collins, M. P., and Will, G. T., "Constitutive model for reinforced concrete finite element analysis," ACI Structural Journal, Vol. 88, No. 1, pp.49-59. 1991.
[24] Kafkalidis, M.S. and Thouless, M.D., "The effects of geometry and material properties on the fracture of single lap-shear joints," International Journal of Solids and Structures, Vol. 39, pp.4367–4383., 2002.